AADE-11-NTCE-69

Thixotropic and Rheopectic Modeling of Xanthan/Borate Gel System

Mehdi Mokhtari, Middle East Technical University*

*Now with Colorado School of Mines

Abstract

Rheological properties of fluids are an essential part of any fluid flow problem and are required to be obtained accurately as well as easily. In this paper, xanthan is crosslinked with borate in order to make a gel which is intended to block lost circulation zones. Thixotropic, shear thinning by time, and rheopectic, shear thickening by time, are behaviours that were investigated by using steady shear viscometry method.

The time-dependency of this gel system is estimated by Weltman model in which viscosity can be obtained at any time under steady shear conditions. The system exhibits a weak thixotropic behaviour up to sol-gel transition time and strong rheopectic behaviour afterwards. The coefficients of Weltman model (1943) are obtained by regression analysis and the goodness of fit values show reasonable fitting between the experimental data and the model.

However the Weltman model is limited due to its dependency on constant shear rate data. Therefore, Tiu and Boger model (1974) was also investigated. This model predicts shear stress as a function of both shear rate and time. It consists of a structural parameter which describes the structure breakdown by time and a rheological model. Zero order kinetic equation was found appropriate for determining the structure parameter and the Herschel-Bulkley model was found to be the best fitting rheological model based on residual mean squares of samples presented by box-whisker plots. A modified low shear yield point model is also suggested for this gel by studying the shear stress at very low shear rate to be substituted in the Herschel-Bulkley model. As a result, the Tiu and Boger model can describe the rheological properties of this gel as a function of time precisely as well as straightforwardly.

Introduction

A considerable amount of Non-Newtonian fluids is consumed in the petroleum industry for a variety of operations such as: drilling fluids circulation, hydraulic fracturing, enhanced oil recovery fluids injection, water shut-off, etc. This extensive application accounts for a substantial cost and makes the science of rheology of real practical importance. Some of these fluids exhibit time-independent behaviour and can be divided in to shear thinning and shear thickening fluids due to their increase or decrease of viscosity by increasing shear rate respectively. The other group is time-dependent materials which are divided in to thixotropic and rheopectic types due to their decrease or increase of viscosity by time respectively.

The xanthan/borate gel system exhibits both thixotropic and rheopectic behaviours at different stages of its life. In the beginning, there is structural breakdown due to shear and magnesium chloride and there is structural build up after sol-gel transition time due to crosslinking of xanthan chains by borate as the crosslinker which will finally lead to a three-dimensional gel structure intended for lost circulation treatment. Mokhtari and Ozbayoglu (2010) investigated the gelation behaviour of this gel system and obtained initial and final gelation time as well as initial and final viscosity and suggested empirical models to predict those parameters. Moreover the effects of concentrations of xanthan blended with borax, magnesium chloride, pH-controller as well as temperature, mixing time, shear history and shear rate were determined.

The hysteresis loop is one of the earliest methods to investigate time-dependent characteristics of fluids. In this method, shear stress is measured in a shear rate increasing manner followed by shear rate decreasing manner. A clockwise figure indicates thixotropic behaviour and counter-clockwise indicates rheopectic behaviour. However, this method shows a very complex shear history of a shear sensitive sample, and the relation between the loop area and the material parameters is complicated (Figoni and Shoemaker 1983, 1984).

Steady shear viscometry is another method in which shear stress is recorded under a constant shear rate condition. The Weltman model (1943) is one of the earliest models to describe time dependency by using steady shear data. Later Hahn et al. (1959), Figoni and Shoemaker (1983) also introduced their models:

Weltman Model:

$$\tau = A - B\ln t \tag{1}$$

Hahn model:

$$\log(\tau - \tau_e) = P - at \tag{2}$$

Figoni and Shoemaker model:

$$\tau = \tau_e + (\tau_{\max} - \tau_e)\exp(-kt) \tag{3}$$

where τ is shear stress at any time, τ_e is shear stress at equilibrium, $\tau_{\max}$ is maximum shear stress and A, B, P, a and k are constants of these equations. The Weltman model is employed extensively in food products engineering: Abu-Jdayil and Mohameed(2003), Choi and Yoo(2004) ,Basu et al.(2007), Cancela et al.(2007) studied the time dependent behaviour of starch-milk-sugar pastes, food suspensions, pineapple jam, and stirred yogurt by the Weltman model respectively. Durairaj et al. (2004) investigated the thixotropy of solder and conductive adhesive pastes. All of these studies report good results in fitting between experimental data and the Weltman model.

However, the Weltman model is restricted to steady shear data and can not provide a rheological model, shear stress as a function of shear rate, which can be later used in fluid flow problems such as calculating pressure loss. The Tiu and Boger model (1974) overcame this limitation. Their model consists of a rheological model (Tiu and Boger recommended the Herschel-Bulkley model for food products) and a structural decay parameter. They also assumed that the decay of the structural parameter with time obeys a second-order kinetic equation.

$$\tau = f(\lambda, \dot{\gamma}) = \lambda(\tau_0 + k\dot{\gamma}^n) \quad (4)$$

$$\frac{\partial \lambda}{\partial t} = -k_1(\lambda - \lambda_e)^2 \quad (5)$$

where τ_0 is yield stress, k is consistency index, $\dot{\gamma}$ is shear rate, n is flow behaviour index, λ is structural parameter which ranges from initial value, λ_0, of unity at zero shear time and decreases finally to an equilibrium value, λ_e. The rate constant in the equation, k_1, should be determined experimentally. Besides Tiu and Boger (1974) who studied the time-dependency of three types of mayonnaise by their model, Butler and McNulty (1994) applied the model for investigating the time-dependent rheological characterization of buttermilk; Dewar and Joyce (2006) characterized the time-dependency of maize starch and maltodextrin thickeners used in dysphagia therapy.

As it was mentioned before, a rheological model is required to be selected for the Tiu and Boger model. Therefore six common rheological models (Bingham-Plastic, Power-Law, Herschel-Bulkley, Robertson-Stiff, Casson, and Sisko) were evaluated to find the best rheological model. An extensive statistical approach was applied to find the best fitting model for the gel system.

1. Power-Law model (De Waele 1923, Ostwald, 1925):

$$\tau = k\dot{\gamma}^n \quad (6)$$

2. Herschel-Bulkley model (1926): $\tau = \tau_0 + k\dot{\gamma}^n$ (7)

3. Bingham-Plastic model (1957): $\tau = \tau_0 + \mu_p \dot{\gamma}$ (8)

4. Sisko model (1958): $\tau = a\dot{\gamma} + b\dot{\gamma}^c$ (9)

5. Casson model (1959): $\tau = (\sqrt{\tau_0} + \sqrt{\mu_\infty \dot{\gamma}})^2$ (10)

6. Robertson-Stiff model (1967): $\tau = A(\dot{\gamma} + \dot{\gamma}_\circ)^B$ (11)

Ratkowsky (1990) emphasized that the use of the goodness of fit, R^2, is misleading for evaluation of non-linear models. Okafor and Evers (1992) studied the Robertson-Stiff model accuracy in comparison to the Power-Law and the Bingham-Plastic models. They discovered that the Robertson-Stiff model can predict the rheological behavior of two types of clay drilling fluids better than those of conventional models. Weir and Bailey (1996) conducted an extensive statistical study on 414 viscometer data in order to find the best rheological model. Twenty rheological models were evaluated. Several other models could exhibit better results than the conventional models. In another study(1998),they investigated the best rotational viscometer readings for direct estimation of parameters of rheological models. Conventional readings were determined to not be appropriate and other default readings such as the 600/30 combination for Bingham-Plastic instead of 600/300 were suggested. Moreover the Sisko model was found to be the best rheological model. Power and Zamora (2003) studied yield stress by vane rheometer. Among six candidates for yield stress measurement(shear stress at 6 and 3 rpm, low shear yield point(LSYP), zero gel strength, initial gel strength and 10 minute gel strength), the LSYP was obtained to be the best representative of yield stress based on the results from vane rheometer. Kok and Alikaya (2004) examined 45 KCL/polymer samples and concluded that the Power-Law is the best fitting model. Kelessidis et al. (2006) applied the golden section search method to obtain yield stress since non-linear regression analysis can lead to meaningless, negative, yield points. Finally, the other parameters of Herschel-Bulkley were obtained by linear regression.

Materials and Procedure

All experiments were performed on a coaxial rotational viscometer with a bob radius of 1.7245 cm, a bob height of 3.8 cm and a rotor radius of 1.8415 cm. A variety of samples were prepared at different concentrations of a blend of xanthan and borax, pH-controller, and magnesium chloride at different temperatures (materials were used as received and they were not pure). Xanthan is the primary polymer of the system and borax is the raw crosslinker. Therefore, the blend is called Poly-Cross. The pH-controller can lead borax to convert to borate ions necessary for crosslinking. Thus, it can initiate and accelerate the crosslinking. Magnesium chloride can reduce

viscosity and rate of crosslinking by consuming borate ions. First of all, the magnesium chloride was mixed with water, followed by adding poly-cross and finally the pH-controller was added. Then the samples were transferred to the viscometer which was already at the desired temperature.

Two sets of experiments were performed. In the first part, steady shear viscometry method was employed in which the viscosity was measured under constant a shear rate of 3 rpm ($5.1069\,s^{-1}$) in order to find the Weltman model's coefficients or the structural decay parameter in the Tiu and Boger model. The second set of experiments were conducted at 10 shear rates(0.1, 1,3,6,50,100,200,300,450,600) in order to find the best rheological model as well as the low shear yield point(LSYP).

Theory

The coefficients of the Weltman model (A, B) were obtained by plotting shear stress, τ, against $\ln t$. The parameter "A" represents the initial stress and parameter "B" is the time-dependent index. A positive value of B determines thixotropic behaviour and a negative value determines rheopectic behaviour. For each of the samples, the goodness of fit, R^2, values in the thixotropic and rheopectic regions were obtained.

In order to find the best rheological model for substituting in the Tiu and Boger model, a statistical approach was applied to several samples. The shear stress at ten shear rates was measured and the data was correlated by six common rheological models. Residual sum of squares, RSS, and residual mean squares, RMS, were calculated:

$$RSS = \sum_{i=1}^{n} [\tau_{mi} - \tau_{pi}]^2 \tag{12}$$

$$RMS = \frac{RSS}{(n-p)} \tag{13}$$

where τ_m, τ_p are measured shear stress and predicted shear stress by models respectively. "n" and "p" are number of data points (10 shear rates in this study), and the number of parameters (2 for Bingham-Plastic, Power-Law, and Casson models and 3 for Herschel-Bulkley, Robertson-Stiff and Sisko models). Finally, the RMS values were depicted in box-whisker plots to find the best rheological model. The box-whisker plots show a non-outlier maximum, 75th percentile, median, 25th percentile, and a non-outlier minimum from top to bottom of the graph.

According to the work of Tiu and Boger, a second order kinetic equation (equation-5) for the decay of structural parameter was first investigated. Apparent viscosity is defined as ratio of shear stress to shear rate:

$$\eta = \frac{\tau}{\dot{\gamma}} \tag{14}$$

Then apparent viscosity can be substituted in equation-4 and will result in:

$$\eta = \frac{\lambda(\tau_0 + k\dot{\gamma}^n)}{\dot{\gamma}} \tag{15}$$

or

$$\lambda = \frac{\eta\dot{\gamma}}{(\tau_0 + k\dot{\gamma}^n)} \tag{16}$$

Now equation-16 should be differentiated and substituted in equation-5:

$$\frac{\partial\lambda}{\partial t} = \frac{\partial\eta}{\partial t}\frac{\dot{\gamma}}{(\tau_0 + k\dot{\gamma}^n)} \tag{17}$$

$$\frac{\partial\eta}{\partial t} = -a_1(\eta - \eta_e)^2 \tag{18}$$

$$a_1 = k_1\frac{\dot{\gamma}}{(\tau_0 + k\dot{\gamma}^n)} \tag{19}$$

Integrating Equation-18 at constant shear rate from $\eta = \eta_0$ at t=0 to $\eta = \eta$ at t=t yields:

$$\frac{1}{\eta - \eta_e} = \frac{1}{\eta_0 - \eta_e} + a_1 t \tag{20}$$

Therefore, a plot of $\frac{1}{\eta - \eta_e}$ against time should yield a straight line with the slope of a_1. Then k_1 can be obtained from equation-19 and finally the structural parameter can be obtained from equation-5. However the second-order kinetic equation did not work for the gel system since the plot was not linear. Therefore, the first-order equation was investigated:

$$\frac{\partial\lambda}{\partial t} = -k_1(\lambda - \lambda_e) \tag{21}$$

Doing the same procedure, we will reach equation-22 at the

end. As a result, the plot of $\ln\left(\frac{\eta-\eta_e}{\eta_0-\eta_e}\right)$ against time, t, should give in a straight line with the slope of "$-k_1$".

$$\ln\left(\frac{\eta-\eta_e}{\eta_0-\eta_e}\right)=-k_1 t \tag{22}$$

However the plot again was not linear, but the plot of $\left(\frac{\eta-\eta_e}{\eta_0-\eta_e}\right)$ against time was found to be linear with a good fit. Therefore, by back calculation, the structural parameter was found to fit the zero-order kinetic equation:

$$\left(\frac{\eta-\eta_e}{\eta_0-\eta_e}\right)=-k_1 t \tag{23}$$

where η_0 is the initial viscosity at time zero and η_e is the final and lowest viscosity of the thixotropic period. Differentiating equation-23 will result in:

$$\left(\frac{1}{\eta_0-\eta_e}\right)\frac{\partial\eta}{\partial t}=-k_1 \tag{24}$$

By substituting equation-15 in the above equation, we will reach:

$$\frac{(\tau_0+k\gamma^n)}{\gamma}\frac{\partial\lambda}{\partial t}=-k_1(\lambda_0-\lambda_e)\frac{(\tau_0+k\gamma^n)}{\gamma} \tag{25}$$

or

$$\frac{\partial\lambda}{\partial t}=-k_1(\lambda_0-\lambda_e) \tag{26}$$

where λ_0 is the structural parameter at time zero and is equal to unity and λ_e is the equilibrium structural parameter or the final point of thixotropic period which is at the lowest viscosity.

Results and Discussions

Table-1 depicts the composition of samples and Tabel-2 shows the coefficients of Weltman's model and the fitness of the model to the experimental data for the forty samples. C_{pc}, C_r, C_A and T are concentration of poly-cross (wt %), accelerator or pH-controller (wt %), retarder or magnesium chloride (wt %) and temperature (°C) respectively. The subscripts of "t" and "R" in Table-2 stands for thixotropic or rheopectic respectively. Figure-1 shows a typical Weltman's graph in which shear stress, τ, is plotted against "$\ln t$"(sample No. 26). First period is a weak thixotropy known also from the low positive "B" values, followed by a strong rheopectic period known also by the high negative "B" values. The R^2 values demonstrate a good fitting between the experimental data and the Weltman's model.

Figure-2 illustrates the plot of "$L_2=\frac{1}{\eta-\eta_e}$", "$L_1=\ln\left(\frac{\eta-\eta_e}{\eta_0-\eta_e}\right)$", and "$L_0=\left(\frac{\eta-\eta_e}{\eta_0-\eta_e}\right)$" versus time in order to find "$-k_1$" for second-order, first order, and zero-order kinetic equation respectively. The graphs for second-order and first-order are not linear and as a result they do not give reasonable results. The y-axis values for the second-order graph are multiplied by 100 in order to be in appropriate scale in the figure in comparison to the other graphs. Zero-order plot illustrates a good fitting straight line and the slope is "$-k_1$"value. The same calculations were performed on other samples, and all confirmed the zero-order kinetic equation to fit the data. Table-3 shows the "$-k_1$" and "R^2" values for different samples. By having "k_1" and integrating equation-26, the structural parameter can be obtained as:

$$\lambda=-k_1(\lambda_0-\lambda_e)t+\lambda_0 \tag{27}$$

Since $\lambda_0=1$, the final structural equation as a function of time can be obtained as:

$$\lambda=1+k_1(\lambda_e-1)t \tag{28}$$

Then the best rheological model should be obtained and associated with the structural parameter in equation-28 can generate a time-dependent rheological model. To this end, shear stress at 10 shear rates for 20 samples was measured. Table-4 illustrates the composition of samples and Figure-3 shows the rheograms. All the samples exhibit shear thinning behaviour. Subsequently the residual mean squares, RMS, were obtained for each sample in six rheological models. The range of RMS values is depicted in box-whisker plot in figure-4 and figure-5 for two-parameter and three-parameter models respectively. The two-parameter models give considerable errors and are not suitable models. Among three-parameter models, Sisko and Herschel-Bulkley both exhibit a good fit. However, the Herschel-Bulkley is selected for substituting in the Tiu and Boger's model since the yield stress parameter in this model can be estimated indirectly and makes the model finally a two-parameter model which is much easier and favoured by the industry. To this end, shear stress at very low shear rate, $0.17023\,S^{-1}$, was measured and was assumed as true yield stress. Next, different empirical models (shear stress at 6 rpm, shear stress at 3 rpm, low shear yield point($LSYP=2\tau_3-\tau_6$) and the yield stress obtained from non-linear regression analysis of the Herschel-Bulkley model)

were examined to predict yield stress. The first 3 models did not give reasonable results. As a result, other coefficients for LSYP model were examined and equation-29 was obtained:

$$MLSYP = \tau_3 - 0.5\tau_6 \quad (29)$$

in which MLSYP is the modified low shear yield point, τ_3 is shear stress at 3 rpm and τ_6 is shear stress at 6 rpm. Figure-6 illustrates the comparison of different yield point models. The MLSYP has a better result since its data points are in good fitting around the y=x line. Finally, the yield stress from these empirical models was substituted in the Herschel-Bulkley model and the RMS values were statistically calculated. Figure-7 illustrates that the modified low shear yield point model works well for this gel system. Therefore, precise results can be obtained in an easier method. Finally, equation-30 is proposed for the rheological models of this gel system:

$$\tau = \left[1 + k_1(\lambda_e - 1)t\right] \times \left[\left(\tau_3 - 0.5\tau_6\right) + k\left(\dot{\gamma}\right)^n \right] \quad (30)$$

Conclusions

The thixotropic behavior of the xanthan/borate gel system before the sol-gel transition time and its rheopectic behavior afterwards were studied by the Weltman model. There is a good fit between the model and the experimental data. However, there is also need for a time-dependent rheological model to determine the flow behavior of the gel before sol-gel transition time when the fluid should be pumped down. To this end, the Tiu and Boger model was evaluated. A zero-order kinetic equation for the structural decay parameter and the Herschel-Bulkley for the rheological model part were found to work well.

References

Bailey, W., Weir, I., "Investigation of Methods for Direct Rheological Model Parameters Determination", Journal of Petroleum Science and Engineering, 1998, 21, 1-13

Kok, M.V., "Determination of Rheological Models for Drilling Fluids (A Statistical Approach)", Energy Sources Part A: Recovery, Utilization and Environmental Effects", 26, 153-165

Kok, M.V., Batmaz, T., Gucuyener, I.H., "Rheological Behavior of Bentonite Suspensions", Petroleum Science and Technology, 2000, Vol. 18, Issue 5&6, 519-536

Kelessidis, V.C., Maglione, R., Tsamantaki, C., Aspirtakis, Y., "Optimal determination of rheological parameters for Herschel–Bulkley drilling fluids and impact on pressure drop, velocity profiles and penetration rates during drilling", Petroleum Science and Technology, 2006, Vol. 53, Issue 3-4, 203-224

Lachemet, A., Touil, D., Belaadi, S., Bentaieb, N., Frances, C., "Rheological Behavior of Raw Cement", Journal of Applied Sciences, 2008, Vol. 8, Issue 19, 3485-3490

Mokhtari, M., Ozbayoglu, E., " Laboratory Investigation on Gelation Behavior of Xanthan Crosslinked with Borate Intended to Combat Lost Circulation", SPE 136094 presented in SPE Production and Operations Conference and Exhibition held in Tunis, Tunisia, 8-10 June 2010

Okafor, M.N., Evers, J.F., " Experimental Comparison of Rheology Models for Drilling Fluids", SPE 24086 presented at Western Regional Meeting held in Bakersfield, California, U.S.A, 30 March-1 April 1992

Power, D., Zamora, M., "Drilling Fluid Yield Stress: Measurement Techniques for Improved Understanding of Critical Drilling Fluid Parameters", AADE National Technology Conference held in Houston, Texas, U.S.A, April 1-3, 2003

Weir, I.S., Bailey, W.J., "A Statistical Study of Rheological Models for Drilling Fluids", SPE Journal, December 1996

Durairaj, R., Ekere, N.N., Salam, B., "Thixotropy Flow of Solder and Conductive Adhesive Pastes", Journal of Materials Science: Materials in Electronics, 2004, 15, 677-683

Choi, Y.H., Yoo, B., "Characterization of Time-Dependent Flow Properties of Food Suspensions", International Journal of Food Science and Technology, 2004, 39, 801-805

Dewar, R.J., Joyce, M.J., "The Thixotropic and Rheopectic Behavior of Maize Starch and Maltodextrin Thickeners Used in Dysphagia Therapy", 2006, Carbohydrate Polymers", 65, 296-305

Basu, S., Shivhare, US, Raghavan, GSV, "Time Dependent Rheological Characteristics of Pineapple Jam", International Journal of Food Engineering", 2007, 3

Cancela, A., Maceiras, R., Alvarez, E., "Characterization of Time-Dependent Behavior of Non Fat and Full Fat Stirred Yogurt", European Congress of Chemical Engineering, Copenhagen, 16-20 September 2007

Butler, F., McNulty, P., "Time Dependent Rheological Characterization of Buttermilk at 5°C", Journal of Food Engineering, 1995, 25, 569-580

Ford, E.W., Steffe, J.F., "Quantifying Thixotropy in Starch-Thickend, Strained Apricots Using Mixer Viscometry Techniques", Journal of Texture Studies, 1986, 17, 71-85

Tiu, C., Boger, D.V., "Complete Rheological Characterization of Time-Dependent Food Products", Journal of Texture Studies, 1974, 5, 329-338

Table 1: Composition of samples

No.	C_{pc}	C_A	C_r	T
1	15	5	0.25	80
2	15	5	0.25	60
3	15	5	0	60
4	15	5	0	80
5	15	5	1	80
6	15	10	0.5	80
7	15	10	0.25	80
8	15	10	0.5	60
9	15	10	0	60
10	15	10	0	80
11	15	15	0.5	80
12	15	15	0.25	80
13	20	5	0.5	60
14	20	5	0.5	80
15	20	5	0.25	80
16	20	5	0	60
17	20	5	0	80
18	20	5	1	60
19	20	10	0.5	40
20	20	10	0.5	60
21	20	10	0.5	80
22	20	10	0.25	40
23	20	10	0.25	60
24	20	10	0	80
25	20	10	1	60
26	20	15	0.5	40
27	20	15	0.5	80
28	20	15	0.25	80
29	20	15	0	60
30	20	15	1	80
31	25	5	0.5	80
32	25	5	0.25	80
33	25	5	0	60
34	25	5	0	80
35	25	5	1	80
36	25	10	0.5	80
37	25	10	0.25	80
38	25	10	0	60
39	25	10	1	80
40	25	15	1	40

Table 2: Weltman's coefficients and goodness of fit

No.	A_t	B_t	A_R	B_R	R_t^2	R_R^2
1	12.85	1.40	-30.58	-13.80	0.94	0.98
2	10.31	0.44	-21.79	-10.26	0.81	0.97
3	14.41	0.31	-156.57	-54.47	0.68	0.88
4	12.86	0.58	-131.92	-51.20	0.75	0.86
5	8.19	0.33	-3.21	-3.76	0.93	0.99
6	13.89	1.09	-11.40	-8.36	0.86	0.86
7	15.05	1.41	-30.04	-15.68	0.94	0.92
8	14.00	0.56	-17.28	-10.60	0.94	0.88
9	17.25	0.30	-32.97	-18.85	0.82	0.93
10	24.56	1.00	-40.05	-27.13	0.72	0.9
11	17.45	1.37	-8.59	-9.60	0.99	0.95
12	17.47	0.69	-23.66	-16.29	0.97	0.89
13	28.51	1.93	-52.89	-23.81	0.9	0.98
14	28.42	1.92	-51.87	-23.57	0.91	0.98
15	36.72	4.91	-147.82	-58.91	0.98	0.99
16	32.63	0.54	- 252.55	-93.25	0.76	0.94
17	43.24	1.72	-252.54	-105.28	0.72	0.93
18	20.84	0.633	- 44.87	-20.15	0.72	0.92
19	39.40	1.07	- 21.82	-18.90	0.95	0.98
20	35.68	0.98	- 38.03	-26.07	0.77	0.96
21	43.51	3.42	- 46.84	- 30.88	0.84	0.95
22	31.50	0.14	- 38.35	-22.93	0.41	0.97
23	33.87	1.46	- 98.42	-44.60	0.78	0.96
24	54.50	-4.29	- 33.44	-42.93	0.87	0.93
25	27.35	2.79	- 71.78	-29.03	0.96	0.76
26	65.02	1.88	21.66	-14.11	0.87	0.99
27	55.11	3.78	- 70.80	-44.55	0.85	0.95
28	53.19	3.07	- 25.96	30.80	0.91	0.95
29	67.47	-1.90	42.31	-14.04	0.71	0.96
30	34.98	1.05	- 7.66	-17.55	0.6	0.98
31	61.61	6.12	- 209.38	-85.61	0.83	0.96
32	83.11	10.60	- 287.06	- 117.71	0.9	0.95
33	85.46	1.97	- 380.5	-147.29	0.51	0.97
34	105.71	4.49	- 97.20	- 75.04	0.87	0.77
35	73.56	9.70	- 72.86	- 40.30	0.99	0.99
36	117.33	15.47	- 5.30	-33.48	0.98	0.98
37	111.26	10.41	- 63.24	-58.7	0.97	0.99
38	121.29	2.58	- 289.80	-150.4	0.57	0.92
39	9345.5	922.43	1700.6	-2092.6	0.9	0.98
40	98.27	1.015	23.96	-25.33	0.56	0.99

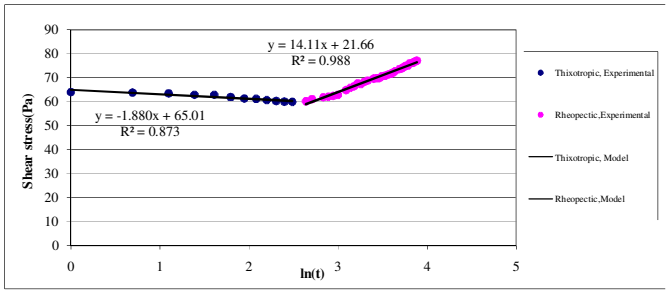

Figure 1: typical Weltman's graph

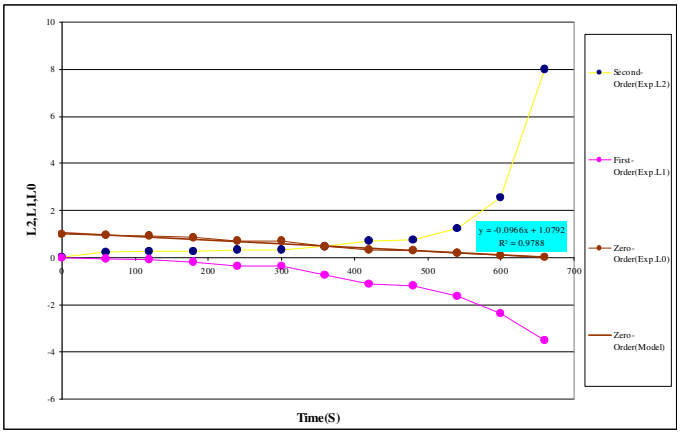

Figure 2: determining the degree of order of the Tiu and Boger's model

Table 3: $-k_1$ and R^2 values for Tiu and Boger's model

Sample	$-k_1$	R^2	Sample	$-k_1$	R^2
1	-0.063	0.95	18	-0.060	0.85
2	-0.043	0.75	19	-0.079	0.95
3	-0.055	0.74	21	-0.113	0.97
4	-0.090	0.92	23	-0.95	0.97
5	-0.081	0.82	25	-0.091	0.96
6	-0.086	0.79	26	-0.105	0.98
7	-0.153	0.92	28	-0.161	0.95
8	-0.075	0.97	31	-0.080	0.99
12	-0.149	0.97	32	-0.084	0.98
13	-0.089	0.92	33	-0.125	0.99
14	-0.066	0.98	35	-0.080	0.98
15	-0.080	0.98	36	-0.149	0.99
16	-0.043	0.89	37	-0.165	0.99
17	-0.119	0.93	39	-0.125	0.98

Table 4: Composition of samples for rheogram tests

	C_{pc}	C_A	C_r	T
Sample	**wt%**	**wt%**	**wt%**	**°C**
1	**15**	**10**	**0**	**80**
2	**15**	**5**	**0**	**60**
3	**15**	**5**	**0**	**80**
4	**15**	**5**	**1**	**80**
5	**15**	**10**	**0**	**40**
6	**15**	**10**	**0**	**60**
7	**15**	**10**	**1**	**40**
8	**15**	**10**	**1**	**60**
9	**15**	**10**	**1**	**80**
10	**15**	**10**	**0**	**80**
11	**15**	**7.5**	**0**	**80**
12	**20**	**5**	**0.5**	**40**
13	**20**	**5**	**0**	**40**
14	**20**	**5**	**0**	**60**
15	**20**	**5**	**0**	**80**
16	**20**	**5**	**1**	**40**
17	**20**	**5**	**1**	**60**
18	**20**	**5**	**1**	**80**
19	**20**	**10**	**1**	**40**
20	**20**	**10**	**1**	**80**

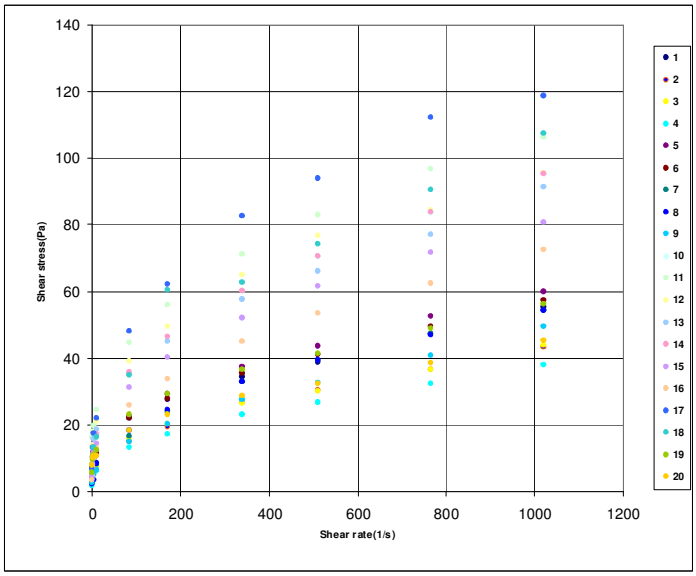

Figure 3: Rheograms of different samples

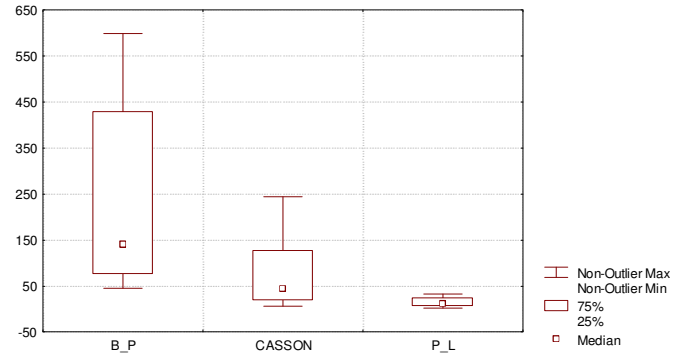

Figure 4: Range of RMS values for Bingham-Plastic (B_P), Casson, and Power-Law (P_L) models

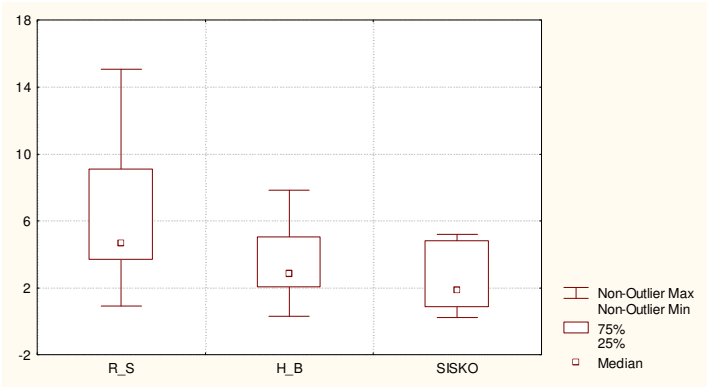

Figure 5: Range of RMS values for Robertson-Stiff (R_S), Herschel_Bulkley (H_B) and Sisko models

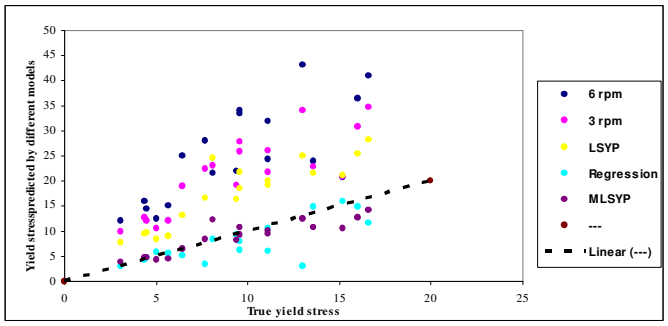

Figure 6: Yield stress determination

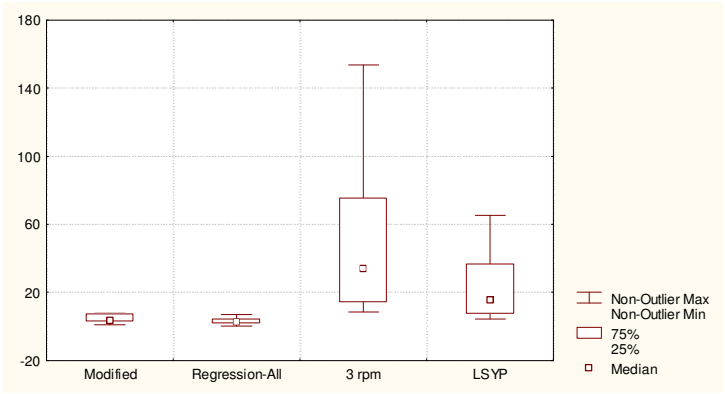

Figure 7: Range of RMS values for yield stress models